Chin. Geogra. Sci. 2015 Vol. 25 No. 6 pp. 713–727
doi: 10.1007/s11769-015-0733-6

Springer Science Press
www.springerlink.com/content/1002-0063

Modeling Hydrothermal Transfer Processes in Permafrost Regions of Qinghai-Tibet Plateau in China

HU Guojie, ZHAO Lin, LI Ren, WU Tonghua, WU Xiaodong, PANG Qiangqiang, XIAO Yao, QIAO Yongping, SHI Jianzong

(*Cryosphere Research Station on Qinghai-Xizang Plateau*, *State Key Laboratory of Cryospheric Sciences*, *Cold and Arid Regions Environmental and Engineering Research Institute*, *Chinese Academy of Sciences*, *Lanzhou* 730000, *China*)

Abstract: Hydrothermal processes are key components in permafrost dynamics; these processes are integral to global warming. In this study the coupled heat and mass transfer model for (CoupModel) the soil-plant-atmosphere-system is applied in high-altitude permafrost regions and to model hydrothermal transfer processes in freeze-thaw cycles. Measured meteorological forcing and soil and vegetation properties are used in the CoupModel for the period from January 1, 2009 to December 31, 2012 at the Tanggula observation site in the Qinghai-Tibet Plateau. A 24-h time step is used in the model simulation. The results show that the simulated soil temperature and water content, as well as the frozen depth compare well with the measured data. The coefficient of determination (R^2) is 0.97 for the mean soil temperature and 0.73 for the mean soil water content, respectively. The simulated soil heat flux at a depth of 0–20 cm is also consistent with the monitored data. An analysis is performed on the simulated hydrothermal transfer processes from the deep soil layer to the upper one during the freezing and thawing period. At the beginning of the freezing period, the water in the deep soil layer moves upward to the freezing front and releases heat during the freezing process. When the soil layer is completely frozen, there are no vertical water exchanges between the soil layers, and the heat exchange process is controlled by the vertical soil temperature gradient. During the thawing period, the downward heat process becomes more active due to increased incoming shortwave radiation at the ground surface. The melt water is quickly dissolved in the soil, and the soil water movement only changes in the shallow soil layer. Subsequently, the model was used to provide an evaluation of the potential response of the active layer to different scenarios of initial water content and climate warming at the Tanggula site. The results reveal that the soil water content and the organic layer provide protection against active layer deepening in summer, so climate warming will cause the permafrost active layer to become deeper and permafrost degradation.

Keywords: permafrost; coupled heat and mass transfer model (CoupModel); soil temperature; soil moisture; hydrothermal processes; active layer

Citation: Hu Guojie, Zhao Lin, Li Ren, Wu Tonghua, Wu Xiaodong, Pang Qiangqiang, Xiao Yao, Qiao Yongping, Shi Jianzong, 2015. Modeling hydrothermal transfer processes in permafrost regions of Qinghai-Tibet Plateau in China. *Chinese Geographical Science*, 25(6): 713–727. doi: 10.1007/s11769-015-0733-6

1 Introduction

Permafrost (defined as ground where temperature has remained at or below 0℃ for a period of least two consecutive years) is a key component of the cryosphere through its influence on energy exchanges, hydrological processes, natural hazards and carbon budgets and hence on the global climate system (Riseborough *et al*., 2008). The permafrost area in China accounts for approximately 10% of the Earth′s permafrost area, the third

Received date: 2013-09-30; accepted date: 2014-01-08
Foundation item: Under the auspices of National Major Scientific Project of China (No. 2013CBA01803), Science Fund for Creative Research Groups of National Natural Science Foundation of China (No. 41121001), National Natural Science Foundation of China (No. 41271081), Foundation of One Hundred Person Project of Chinese Academy of Sciences (No. 51Y251571)
Corresponding author: ZHAO Lin. E-mail: linzhao@lzb.ac.cn

largest amount of the world. There is approximately 1.4×10^6 km^2 of permafrost in the Qinghai-Tibet Plateau, covering 54.3% of the entire Plateau area (Cheng and Zhao, 2000). The freezing of the soil is a very complex process; it is accompanied by the migration of water and water phase transition, heat transmission and solute transport (Xu *et al*., 2001). Transfer of moisture and heat is an important part during the soil freezing and thawing process and plays an extremely important role in agriculture, water resources, environment and infrastructure (Cheng, 1990). The simulated migration process of soil moisture and heat is very important to global climate change research in the Qinghai-Tibet Plateau (Yang and Yao, 1998; Wu *et al*., 2003; Zhao, 2004). It is essential to improve the simulation accuracy of the land surface process by modeling hydrothermal processes well (Henderson-Sellers *et al*., 1993; Loumagne *et al*., 1996; Zhang Yanwu *et al*., 2003). Some land-surface process models have been used to study the frozen soil water-heat processes in permafrost regions of the Qinghai-Tibet Plateau of China (Yang *et al*., 2000; Wu *et al*., 2003; Zhang Yu *et al*., 2003; Gao *et al.*, 2004; Wang and Shi, 2007; Luo Siqiong *et al*., 2008). However, little is known about the land surface processes in permafrost regions of the Qinghai-Tibet Plateau of China (Wang and Shi, 2007). The permafrost of the plateau is more sensitive to climate and surface conditions (Cheng, 1998). Therefore, studying the soil freeze-thaw changes could improve our knowledge to understand the interaction between soil freeze-thaw events and climate change.

In recent years, hydrothermal coupling experiments and models have made progress for hydrothermal processes in the permafrost region (He *et al*., 2001; Mao *et al*., 2003; Luo Jinming *et al*., 2008) in terms of developing a common model that can be adapted to various conditions (Li *et al*., 2008), but have more focused on ice, frost action engineering and land surface processes with a numerical atmosphere model. A number of different numerical models, such as Harlan (1973), coupled heat flow and moisture flow model (FROSTB) (Shoop and Bigl, 1997), simultaneous heat and water (SHAW) (Nassar *et al*., 2000; Zhao *et al*., 2008) and community land model (CLM3) (Alexeeve *et al*., 2007; Nicolsky *et al*., 2007), have been developed to study frozen soil water-heat processes. However, most of the modeling studies were conducted in high-latitude regions (Henderson-Sellers *et al*., 1995; Bowling *et al*., 2003), and few were carried out in the Qinghai-Tibet Plateau region. In such a low-latitude alpine region, the characteristics of solar radiation, air temperature, wind speed, and snow cover are different from those at high-latitude regions (Xiao *et al*., 2013). The soil-vegetation-atmosphere system (SVAT) model called CoupModel has been widely used in modeling water-heat processes in soil (Zhang *et al*., 2007; Scherler *et al*., 2010; Wu *et al.*, 2011a; 2012; Zhou *et al*., 2013). It only used heat and water transfer processes in the frozen alpine meadows of the source area of the Heihe River in Northwest China (Yang *et al*., 2010).

Hydrothermal transfer processes play an important role in energy change and climate change, however, there is a lack of studies on these processes in the Qinghai-Tibet Plateau. Therefore, further study on the hydrothermal characteristics of the permafrost active layer in the Qinghai-Tibet Plateau is necessary. In this study, the CoupModel was used to simulate the hydrothermal transfer processes and perform sensitivity analysis of the active layer change in the Qinghai-Tibet Plateau. The objectives of this study are to: 1) simulate soil temperature and moisture and soil heat flux and analyze their effectiveness compared to the measured values; 2) describe the general behavior of soil heat flux and hydrothermal transfer processes based on the simulation results; and 3) predict and demonstrate the effect of increasing air temperature, initial water content and organic layer depth on active layer thickness.

2 Study Area and Data

2.1 Study site

The Tanggula observation site (33°04′N, 91°56′E), with an altitude of 5100 m, is situated on a gentle slope in the Tanggula Range Passon the Qinghai-Tibet Plateau in China (Fig. 1). The site was set up on a southwest-facing gentle slope on the eastern bank of the Dam River near the Qinghai-Tibet Highway (QTH) in the Tanggula region, and the site was approximately 1 km from the river (Yao *et al*., 2008). It is located in the continuous permafrost zone and is an alpine grassland steppe. The vegetation is alpine meadow distributed in clusters with heights of less than 10 cm and coverage of approximately 20%–30%. The observation site was established in June 2004.

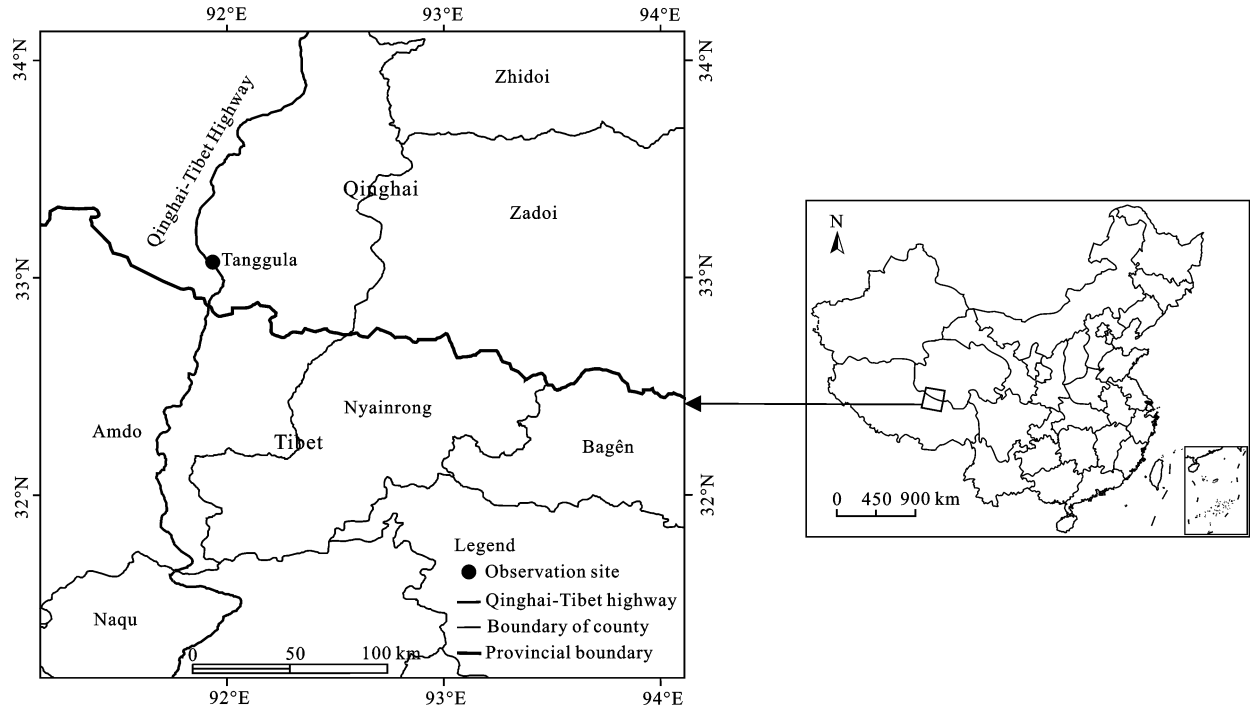

Fig. 1 Location of Tanggula observation site

2.2 Data sources

2.2.1 Site data

Meteorological data consisting of the precipitation, radiation, air temperature, wind speed and relative humidity were recorded hourly with a CR23X data acquisition instrument (Campbell Scientific Inc., USA) at the Tanggula observation site in China. Air temperature, relative humidity and wind speed were measured at heights of 2 m, 5 m and 10 m. Radiation (R_n) was measured by a NR-1/Kipp & Zonen Net radiometer with an error of ± 10% (Table 1). Ground heat flux (G_s) was measured at 5 cm, 10 cm and 20 cm below surface by an HFP01SC with an accuracy of ±3 % (Table 1). Air temperature (T_a) was measured by an HMP45C Tem sensor with an accuracy of ±0.5℃ (Table 1). The soil temperature in the active layer were measured from ground surface to 3 m with a 105T thermocouple Probe with an accuracy of ±0.5℃ (Table 1). The soil moisture content was measured by a Hydra soil moisture sensor with an accuracy of ±2.5% (Table 1). All these sensors were attached to a CR23X data logger (Campbell Company, USA). The time zone was set to Beijing standard time. The soil temperature and moisture were recorded every 0.5 h by a CR1000 data acquisition instrument at different depths in the active layer at the Tanggula observation site.

Table 1 Observation instruments and parameters at Tanggula observation site

Parameter	Instrument	Manufacturer	Error	Depth/Height
Soil temperature	105T	Campbell, USA	±0.5℃	2, 5, 10, 20, 50, 70, 90, 105, 140, 175, 210, 245, 280, 300 cm
Ground heat flux	HFP01SC	Campbell, USA	±3%	5, 10, 20 cm
Soil moisture content	CS616L	Campbell, USA	±2.5%	5, 10, 20, 35, 70, 105, 140, 175, 210, 245, 280, 300 cm
Radiation	CNR-1	Kipp&Zonen, Holland	±10%	2 m
Air temperature	HMP45C	Vaisala, Finland	±0.5℃	2, 5, 10 m
Air humidity	HMP45C	Vaisala, Finland	±0.04%	2, 5, 10 m
Wind speed	05103-L/RM	Campbell, USA	±0.3 m/s	2, 5, 10 m
Snow depth	SR50-L	Campbell, USA	1 cm	2 m
Precipitation	T-200B	Geonor, Norway	0.1 mm	1.5 m

2.2.2 *Atmospheric forcing data*

This study was carried out from 1 January 2009 to 31 December 2012. The atmospheric forcing data used as the driving variables in the simulations presented here were daily air temperature, relative air humidity, wind speed, precipitation, radiation and surface soil temperature. Atmospheric forcing data include air temperature (℃), wind speed (m/s), relative humidity (%), precipitation (mm), snow depth (cm), and global solar radiation (w/m^2), all measured at the Tanggula observation site in China. The mean annual air temperature was −5.1℃, −4.1℃, −4.7℃ and −5.0℃ in 2009, 2010, 2011 and 2012, respectively. Precipitation is normally concentrated in the period from May to September. The minimum air temperature was −22.9℃, −22.7℃, −20.8℃ and −22.2℃, and the maximum was 7.5℃, 10.2℃, 8.1℃ and 9.3℃ in each year. The average daily precipitation and the amount of snow precipitation were measured during 2009−2012. Air temperature, relative humidity and wind speed collected at 2 m were used. The active soil layer thickness is approximately 3 m at the site.

2.2.3 *Surface parameters*

In the model, some parameters have a default value, but many parameters, such as latitude, slope, surface roughness, annual air temperature amplitude (TempAirAmpl), annual mean air temperature (TempAirMean), Albedo, the temperature difference between the air and the precipitation (TempDiffPrec_Air), initial temperature, initial water content, surface temperature, heat flux, *etc*., were calibrated. The samples were analyzed in the laboratory to determine the soil bulk density and soil texture with respect to sand, silt, and clay (Table 2).

Table 2 Soil texture parameters used as inputs for CoupModel

Soil depth (cm)	Sand (%)	Silt (%)	Clay (%)
0–2	85	10	5
2–5	85	10	5
5–9	75	18	7
9–17	70	18	12
17–29	65	22	13
29–49	85	10	5
49–83	85	10	5
83–138	95	3	2
138–230	90	5	5
230–380	68	20	12
380–628	95	3	2

(1) Surface temperature calculation

In the soil depth of 0–5 cm, the soil temperature was measured at 2 cm and 5 cm at the Tanggula observation site. The thickness of the soil is relatively low from the surface to 5 cm, and the soil texture is uniform. Soil temperature changes can be found as linear, and the gradient is the same throughout the area. In this case, surface temperature is estimated as described previously (Zhao *et al*., 2008) as:

$$\Delta T_1/\Delta Z_1 = \Delta T_2/\Delta Z_2 \tag{1}$$

$$T_0 = (5T_{s2} - 2T_{s5})/3 \tag{2}$$

where $\Delta T_1 = T_{s2} - T_0$, $\Delta Z_1 = 0.02$, $\Delta T_2 = T_{s5} - T_{s2}$, $\Delta Z_2 = 0.03$; T_0 is the surface temperature; and T_{s2} and T_{s5} are the soil temperature at 2 cm and 5 cm depths, respectively.

(2) Surface heat flux calculation

The surface heat flux (G_0) is calculated as the following:

$$G_0 = G_z + C_s \int_0^z \frac{\partial T}{\partial t} dz \approx G_z + C_s \frac{\Delta T}{\Delta t} z \tag{3}$$

where z is the soil depth of 5 cm; G_z is the soil heat flux measured at 5 cm depth; T is the soil temperature at 5 cm depth; t is the time and C_s is the volumetric soil heat capacity (J/(m^3·K)). In the northern Qinghai-Tibet Plateau, C_s is taken as 1.18×10^6 (J/ (m^3·K)) (Xiao *et al*., 2011).

3 Methods

3.1 Model description

The CoupModel is a one-dimensional Soil-Vegetation-Atmosphere transfer (SVAT) model that simulates fluxes of water, heat, carbon and nitrogen in the soil-plant-atmosphere system (Jansson and Moon, 2001; Jansson and Karlberg, 2004), coupling the former SOIL (McGechan *et al*., 1997) and SOILN (Eckersten *et al*., 2001) models. The CoupModel is a fairly complex model that simulates water and heat processes in the soil based on well-known physical equations. Two coupled differential equations for water and heat flow represent the core of the model based on the quality of water and energy conservation.

An important advantage of the model is using limited input data to obtain more reasonable and satisfactory simulation results (Jansson and Karlberg, 2004). The

important heat and moisture modules used in this study are described below:

(1) Soil heat process

Soil heat flow is expressed as the sum of conduction, the first term, and convection, the last two terms as follows:

$$q_{\mathrm{h}} = -k_{\mathrm{h}} \frac{\partial T}{\partial z} + C_{\mathrm{w}} T q_{\mathrm{w}} + L_{\mathrm{v}} q_{\mathrm{v}} \tag{4}$$

where q_{h}, q_{w} and q_{v} are heat, liquid water and vapor fluxes, respectively; k_{h} is thermal conductivity; T is soil temperature; C_{w} is liquid water heat capacity; L_{v} is the latent heat of vaporization; and z is depth.

(2) Soil water flow

Soil water flow is assessed to obey Darcy′s law generalized for unsaturated flow by Richards (Jansson and Karlberg, 2004) as follows:

$$q_{\mathrm{w}} = -k_{\mathrm{w}} \left(\frac{\partial \psi}{\partial z} - 1 \right) - D_{\mathrm{v}} \frac{\partial c_{\mathrm{v}}}{\partial z} \tag{5}$$

where k_{w} is the unsaturated hydraulic conductivity; ψ is the water tension; z is depth; c_{v} is the concentration of vapor flow; and D_{v} is the diffusivity coefficient for vapor in the soil.

For surface energy balance, heat flux to the soil is calculated according to the following:

$$q_{\mathrm{h}} = k_{\mathrm{h}} \left(\frac{T_{\mathrm{s}} - T_1}{\Delta z_1 / 2} - 1 \right) + L q_{\mathrm{v,s}} \tag{6}$$

where k_{h} is the thermal conductivity of the topsoil layer; T_{s} is the soil surface temperature; T_1 is the temperature of the middle of the uppermost soil compartment; $\Delta z_1/2$ is the depth of the uppermost soil compartment; and $Lq_{\mathrm{v,s}}$ is the latent water vapor flow from the soil surface to the central point of the uppermost soil layer.

3.2 Model application

The model input data include the site data and atmospheric forcing data and surface parameters of the study area. To obtain better simulation results of changes in permafrost, we increased the number of soil layers to 30, extending the model bottom to a depth of 17 m. The simulated soil profile (0–17 m) was composed of 30 soil compartments, including 17 soil compartments from 0 cm to 400 cm and 13 soil compartments every meter from 4 m to 17 m. This study only analyzed the hydrothermal transfer processes at the depth of 300 cm because the processes are evident in the active layer and exhibit less change at lower depths.

The root mean square error (RMSE) was used to evaluate the simulation results. It reflects the average deviation between the simulated and the measured values and is higher than or equal to zero. Zero indicates that the simulated results do not have error. The determination coefficient (R^2) of the linear regression between simulated and measured values, and the mean error (ME) (Equation (7)), were used in this study.

$$ME = \frac{1}{S} \sum\nolimits_{\mathrm{t}=1}^{S} (y(t) - \hat{y}(t)) \tag{7}$$

where S is the number of samples, $\hat{y}(t)\,(t = 1, 2, \cdots, S)$ is the measured value, and $y(t)\,(t = 1, 2, \cdots, S)$ is the simulated value.

4 Results and Analyses

4.1 Simulated soil temperature

The model predicted the soil temperature for all treatments reasonably well during the course of the 4-year experiment from January 2009 to December 2012. The model appears to overestimate soil temperature during the period from early May to mid-September and underestimate the soil temperature from early January to April every year at soil depths below 140 cm (Fig. 2 with representative depth). We attribute this result to the more complex soil properties at this site.

The simulated soil temperature is comparable to the measured one throughout the entire soil profile (Table 3). However, the error between the simulated and measured soil temperature increases with profile depth. For example, the RMSE generally increases from the top to the 210 cm soil layers. From 0 cm to 105 cm, the R^2 was very close to 1, and the RMSE was less than 1, indicating that the simulated results agreed with the measured ones. In the 140−300 cm layer, the simulation accuracy decreased, but the R^2 was higher than 0.93, the RMSE was less than 1.50, and the ME was less than 1.00. Overall, the average of R^2, RMSE and ME were 0.97, 0.71 and 0.59, respectively, indicating that the simulated soil temperature is accurate.

4.2 Simulated soil moisture

The model predicted the soil moisture well during the period of the 4-year experiment. The simulated results

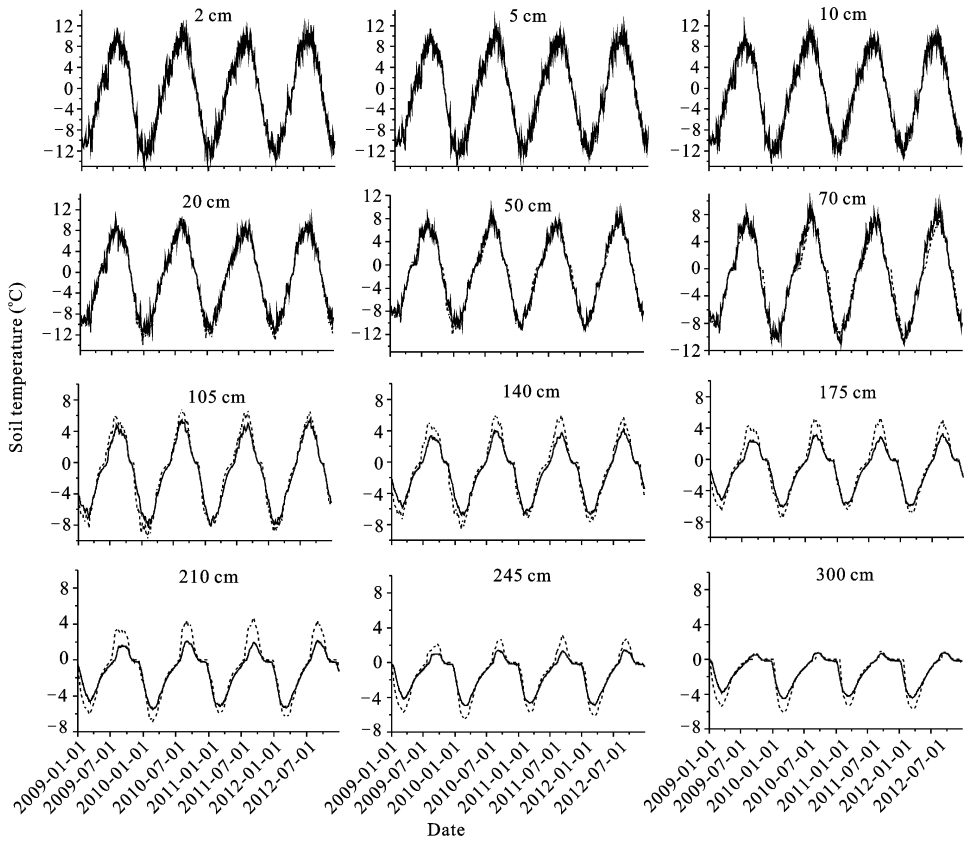

Fig. 2 Measured soil temperature (dashed line) and simulated soil temperature (solid line) at different depths

Table 3 Comparative analysis of simulated and measured soil temperature at different depths

Soil depth (cm)	R^2	ME	RMSE
0	0.99	0.00	0.34
2	0.99	–0.10	0.33
5	0.99	–0.25	0.43
10	0.99	–0.20	0.41
20	0.99	–0.32	0.58
50	0.99	0.99	0.63
70	0.97	0.97	0.99
90	0.98	0.98	0.68
105	0.98	0.98	0.86
140	0.98	0.98	1.04
175	0.97	0.97	1.01
210	0.96	0.96	1.11
245	0.96	0.96	0.82
280	0.95	0.95	0.73
300	0.93	0.93	0.70

Notes: R^2 is the determination coefficient of the linear regression; ME is the mean error; and RMSE is the root mean square error

were consistent with the observations at the depths of 5−20 cm, but they were lower than the measured values in the freezing period. The simulated results at the depths of 35−280 cm were better than those at the surface (Fig. 3). In the 300 cm layer, the measured soil water content increased significantly and suggested that the deep soil moisture conditions were better than the surface, but the simulated results were lower than the measured ones; this result may be due to the selection of the hydraulic property and soil parameters.

4.3 Simulated hydrothermal transfer processes

Soil heat flux can reflect the thermal characteristics of the soil. The surface heat flux (0 cm) was calculated according to Equation (3). The heat flux of 0–20 cm soil layer was simulated, and the simulated values had a large fluctuation (Fig. 4). In the 0–20 cm layer, the R^2 were 0.674, 0.808, 0.881 and 0.904, respectively. The RMSE were 8.67, 6.56, 5.21 and 4.46 at the depth of 0 cm, 5 cm, 10 cm and 20 cm, respectively.

The R^2 between simulated and measured values ranged from 0.52 to 0.90 (Table 4). In most cases, the model predicted higher water contents than the measured values.

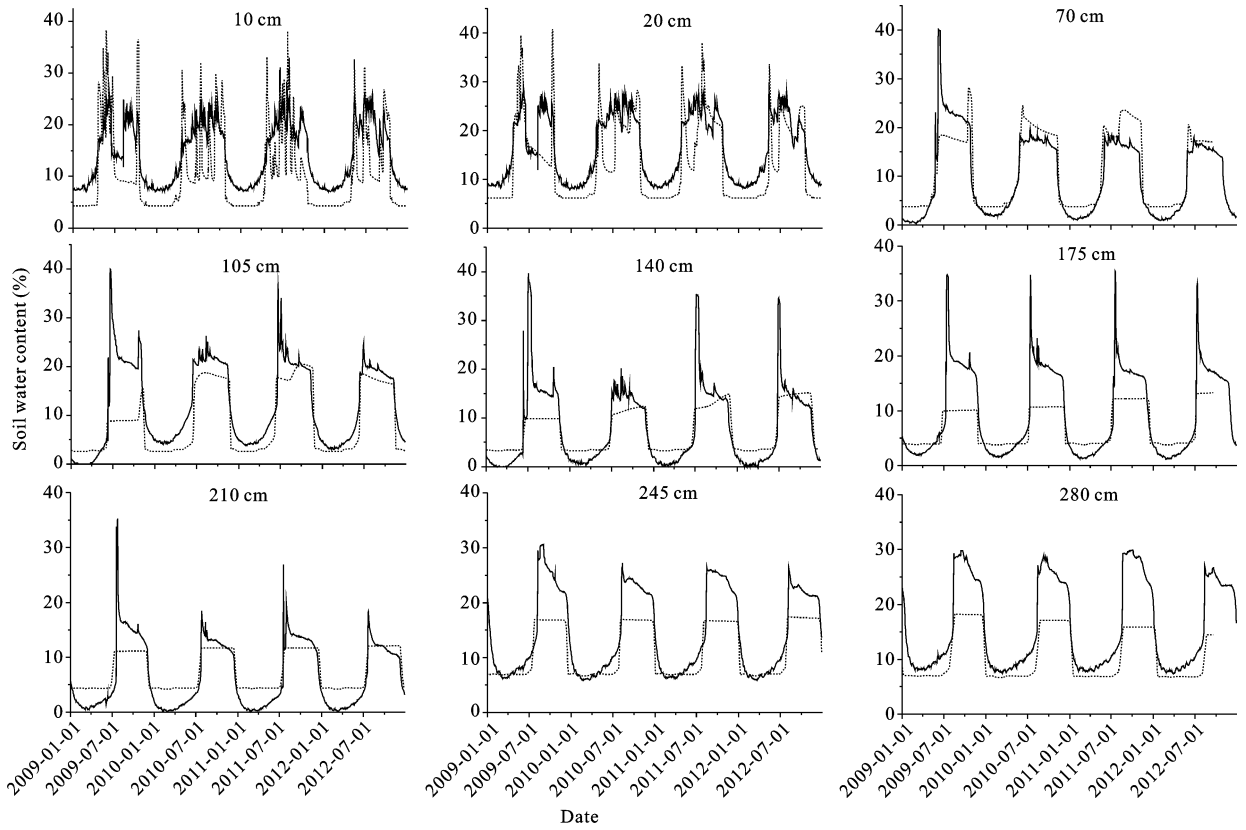

Fig. 3 Simulated (solid line) and measured (dashed line) soil moisture at different depths

Table 4 Comparative analysis of simulated and measured soil moisture at different depths

Soil depth (cm)	R^2	ME	RMSE
5	0.52	–2.09	6.87
10	0.55	–3.84	6.44
20	0.68	–2.99	5.52
35	0.69	6.48	7.82
70	0.79	1.39	3.97
105	0.70	–3.24	5.64
140	0.66	–0.52	5.03
175	0.80	–2.12	5.11
210	0.85	0.95	3.32
245	0.88	–3.22	4.80
280	0.90	–5.21	6.60
300	0.76	–7.02	9.04

The simulated soil moisture in the depths of 20−280 cm showed good agreement with the measured values. The accuracy was lower in the 5 cm and 10 cm layers. Overall, the average of R^2, RMSE and ME were 0.73, 5.85 and −1.79, respectively; and the error between the model simulation and observations on soil moisture was considered to be acceptable.

Based on the calibrated model, an investigation into the hydrothermal transfer process in the active layer was conducted by modeling the soil heat flux process profile and soil moisture movement at different depths. Figure 5 shows that the soil heat flux fluctuates greatly at shallow depths, and as the depth increases, the change stabilizes. When the upper ground temperature is higher than the sublayer, the soil heat conduction movement is from the top to the bottom; when the lower ground temperature is higher than the top, the soil heat conduction is in the opposite direction. The ground soil heat flux gradually changes from positive to negative when the soil starts to freeze at the end of September, indicating that the soil absorbed heat from the outside change into releasing heat, and the process was delayed as depth increasing. In contrast, the ground soil heat flux gradually changes from negative to positive when the soil begins to thaw in early May, showing that the soil released heat into the outside. In the two processes, all the soil depths have a steady, relatively lower (near zero) soil heat flux because soil heat conduction transfer is from the top to the bottom during the freezing period, while the upper soil temperature produces a downward heat conduction during

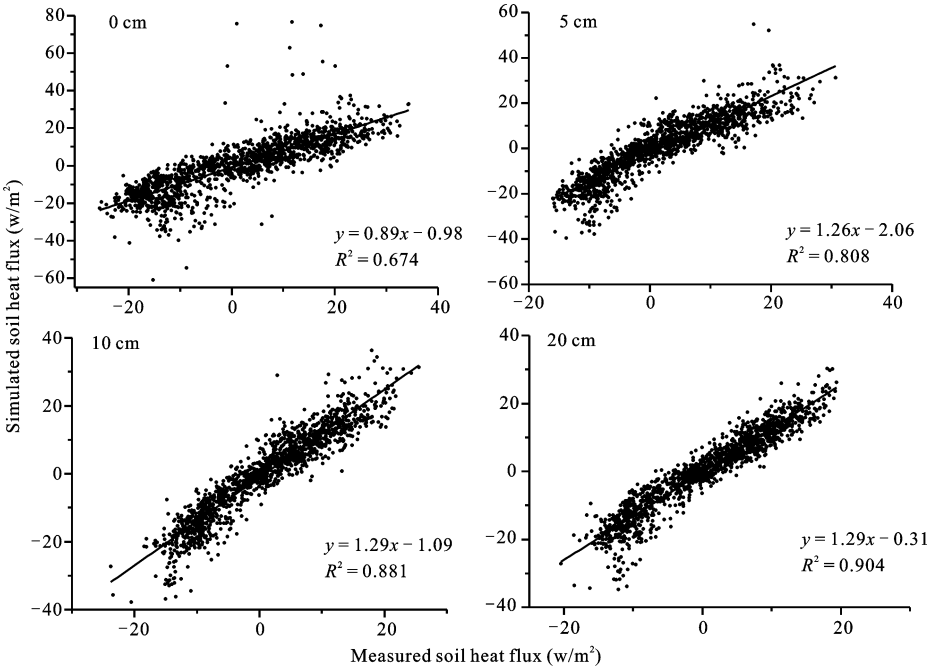

Fig. 4 Simulated soil heat flux in soil layer of 0–20 cm

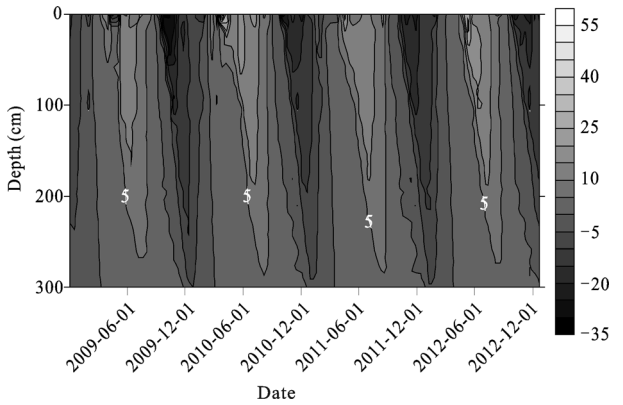

Fig. 5 Soil heat flux (w/m^2) transfer process in active layer

thawing, so the two parts cancelled each other out. After the soil freezes at the end of October, the soil heat flux depends only on the temperature of the upper and lower layer. When the soil thaws in late August, the soil heat flux greatly changes. Overall, the soil heat flux transfer becomes lower with increased depth; and it is low in winter and high in summer.

As seen in Fig. 6, higher soil moisture movement values occur in the rainy season, July and August, at 10 cm and 50 cm depths. When there is heavy precipitation, the shallow soil moisture movement and precipitation have a direct relationship, based mainly on downward flow (Fig. 7) and a large amount of soil infiltration. When the soil is completely frozen, the soil flux is basically zero, and only a few hours appear to exhibit small fluctuations from July to May because of precipitation and evaporation. At the beginning of the thawing process, the soil water content increased, which caused an increase in the downward transmission process. At 105 cm depth, the soil moisture movement undergoes a different transmission process. When the soil starts to freeze, the upper soil layer can absorb moisture from the next layer to freeze completely, resulting in an increased upward soil flux; the upper soil layer can absorb the water and transmit the heat to the lower soil layer. The heat released by the freezing liquid results in a sharp increase in the heat flux. After freezing, the soil moisture does not change, and the soil heat flux is only subject to the temperature of the upper and lower layers. When the soil starts to thaw, it does not show the changes at the surface because the deeper soil layers are not sensitive to evaporation, to the vertical direction of water movement and so on. There is an upward movement of soil water at 175 cm, 210 cm, and 280 cm depths during the freezing period, indicating that the soil water movement in the upper layer can influence the depth of freezing, but the impact is small. Hydrothermal transfer variation with increased depth can be seen; the closer to the surface, the more frequent water movement. It is slower as depth increases, and there is also zero flux in the absence of freezing conditions, with

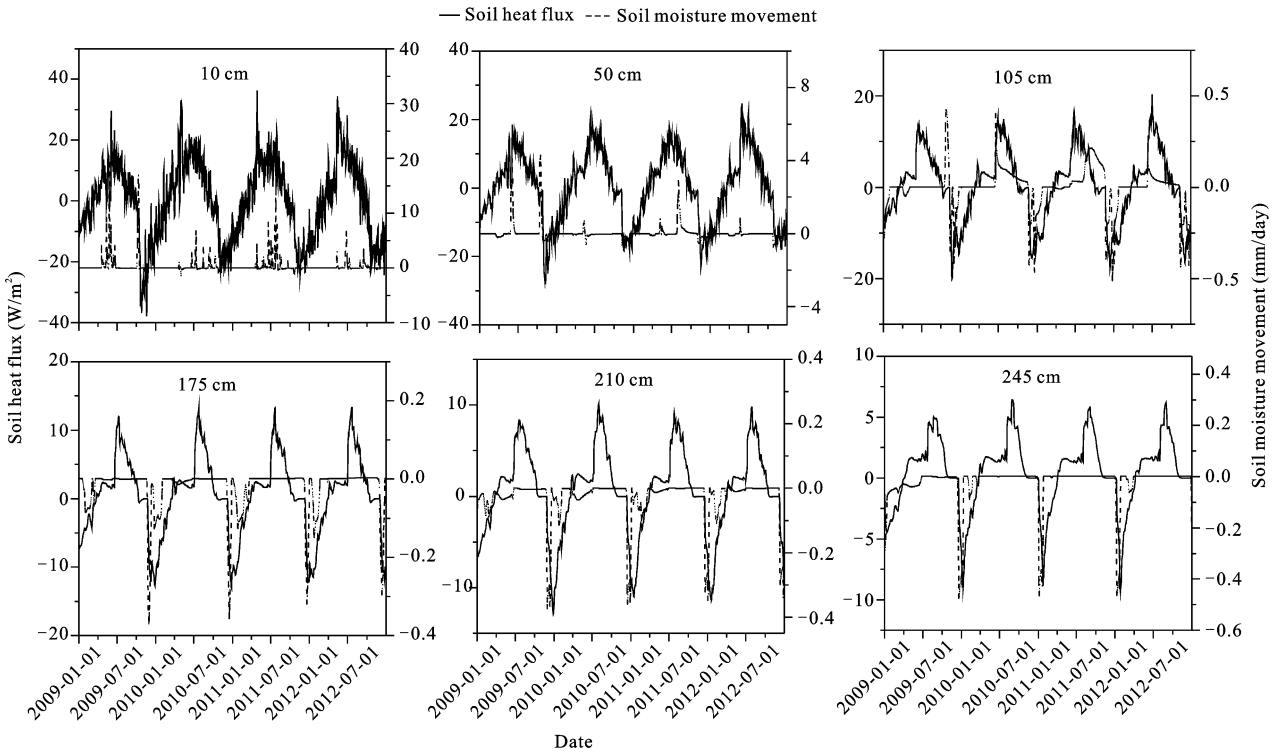

Fig. 6 Simulated heat flow (solid line) and water flow (dashed line) at different depths

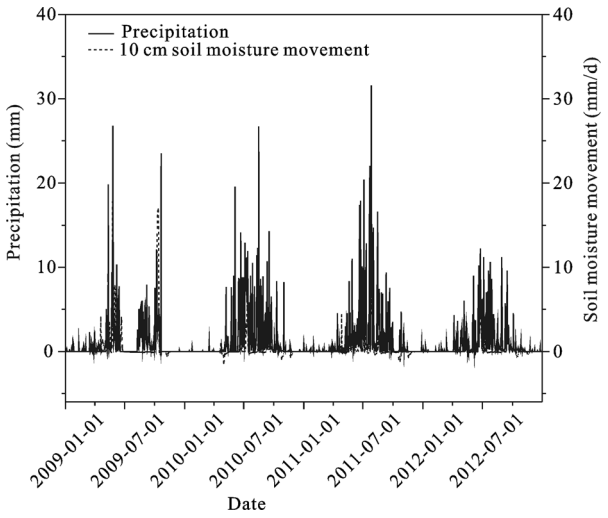

Fig. 7 Precipitation and soil water flow at 10 cm depth

minimal water movement. As the depth increases, it takes longer for the water to reach the lower layers, so these layers freeze more slowly. The time is also increased because soil moisture and soil temperature transmission speed decrease with depth, and the soil particles are coarse.

4.4 Sensitivity analyses

Using the calibrated model, an investigation into the influence of the initial water content on the active layer was conducted by comparing the simulated soil temperature profiles under three different initial water contents (Fig. 8). The initial soil water content at this study site is 0–10%. When it is 0, the active layer thaw depth is similar to the actual depth, but the temperature contour changes differ significantly; and the lowest and highest values are higher than the actual ones at the 0–200 cm depth in particular, suggesting that the temperature decrease is small and it can affect deep soil. Simultaneously, the simulated surface heat flux is slightly lower than the actual in both the freezing and thawing periods. When the initial moisture content increases to 15% and 20%, the active layer thickness was significantly lower, 300 cm and 280 cm, respectively. During thawing periods, the surface heat flux, which is the heat transfer from the atmosphere into the soil and the same occurred in freezing periods, but the active layer thickness was lower (Fig. 9) because of the higher initial water content which delays and reduces the soil heat flux transfer. The initial water content significantly affects the simulated water and heat transfer on the permafrost.

The comparison of simulated soil isothermals from January 1, 2009, to December 31, 2012, for different organic layer depths is shown in Fig. 10. There is no

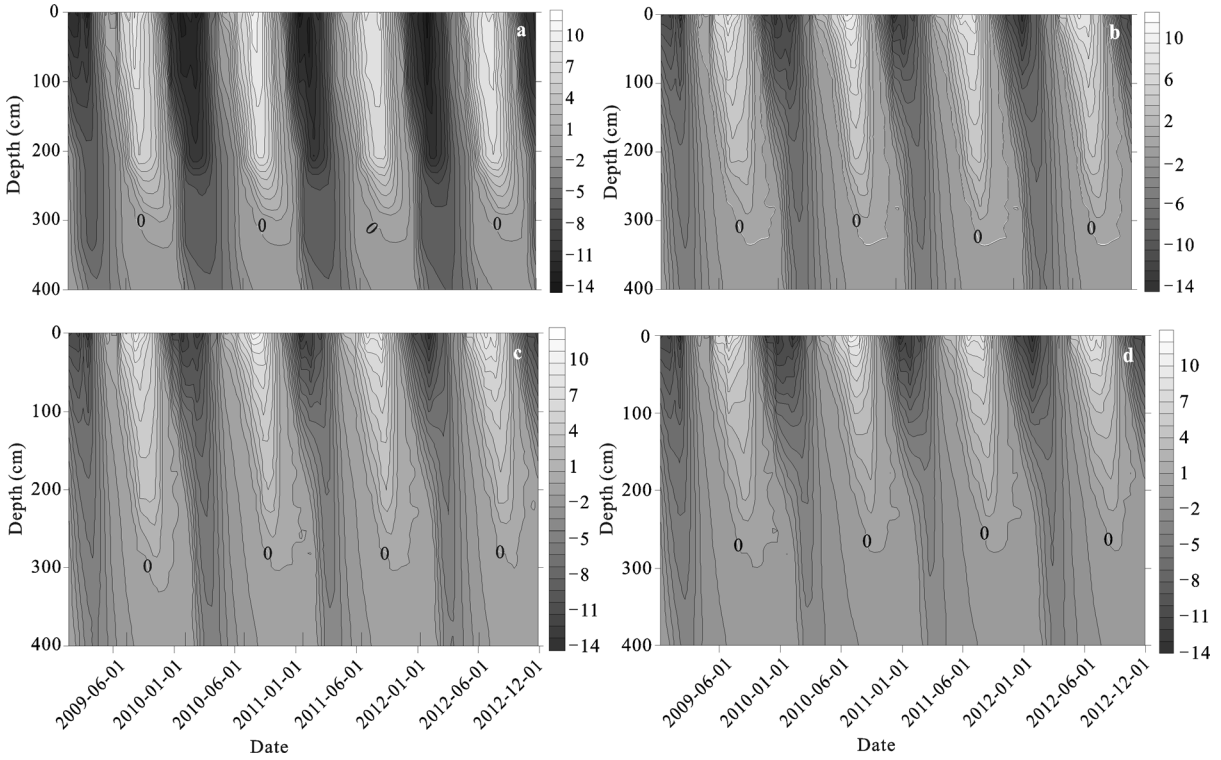

Fig. 8 Simulated isothermals (℃) of soil profile for different initial water content scenarios. a, 0; b, original; c, 15%; d, 20%

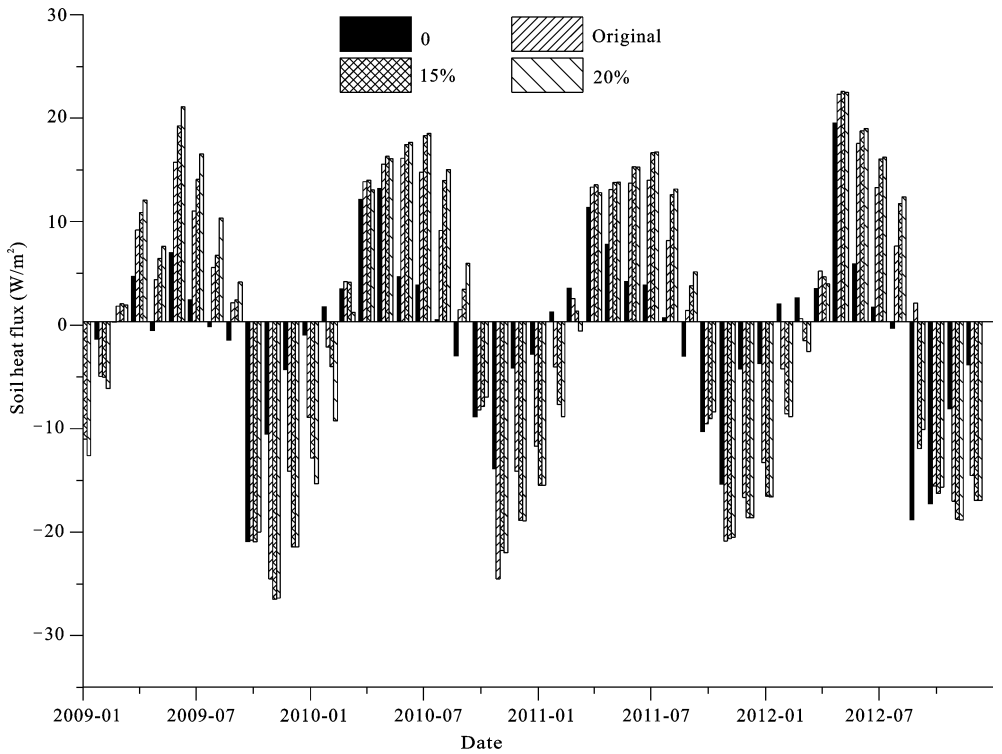

Fig. 9 Simulated monthly average ground heat flux for different initial water content scenarios

organic layer in the Tanggula observation site, and the maximum thawing depth for the active layer in summer is close to 330 cm when the organic layer is 0 cm. However, it is lower than 280 cm and 250 cm with organic layers of 20 cm and 40 cm. The simulated thawing depth gradually decreases with increased organic soil

layer depth. The simulated isothermals in winter move upward with the increase in the depth of the soil organic layer. The simulated monthly average ground heat flux decreased from April to September and indicated that the energy transfer from the atmosphere into the soil decreased (Fig. 11). It can be found that the 40 cm organic soil layer more significantly reduced energy transfer than 20 cm. In March, there is a different variation, even exhibiting opposite changes. The cause of changes may be that the soil heat flux changes the release into the absorption, while the presence of an organic soil layer delays this process. The amount of energy released from the organic soil layer is low from October to November and increases from December to the following February. At the beginning of the thawing period, there is a rapid increase in December in the case of a 20 cm organic soil layer, but the change is more gradual in the case of a 40 cm organic soil layer. The cause of these phenomena is low thermal conductivity. In summary, the soil organic layer reduces the response of the active layer to external factors and contributes to the conservation of permafrost.

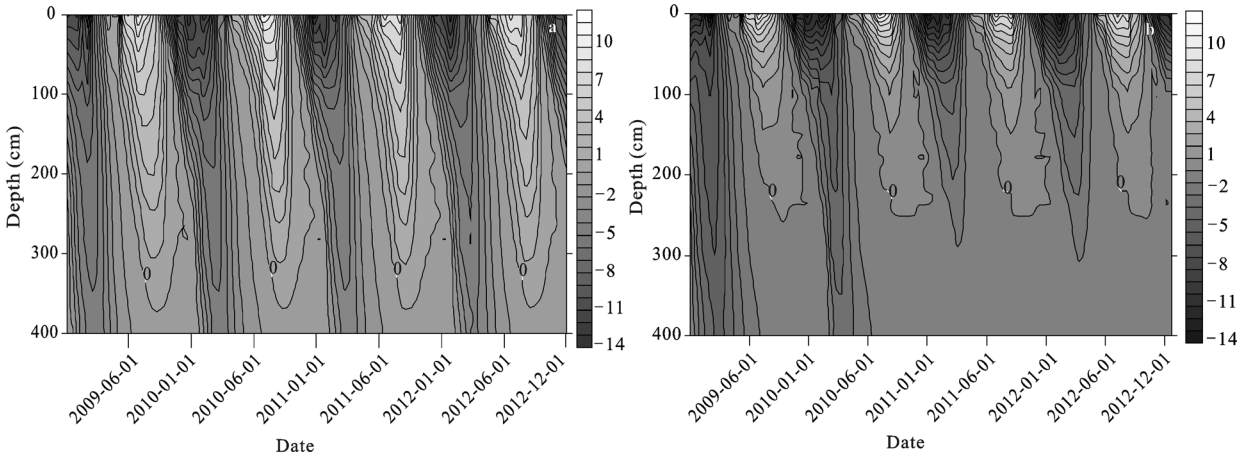

Fig. 10 Simulated isothermals (℃) of soil profile for different organic layer depths. a, 20 cm; b, 40 cm

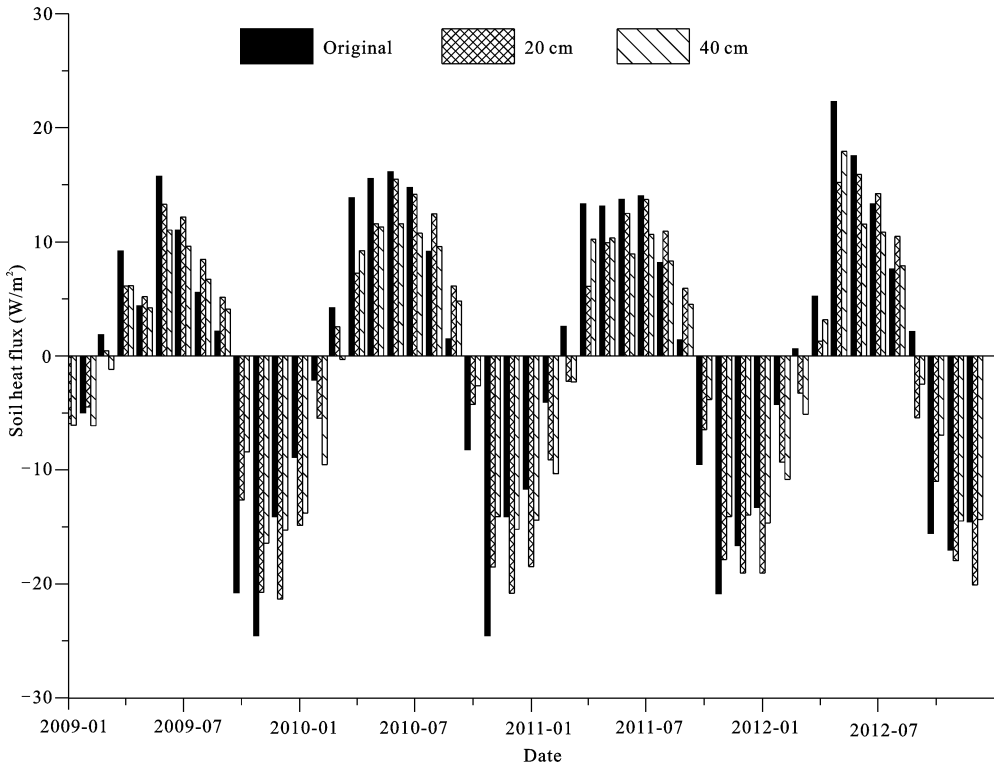

Fig. 11 Simulated monthly average ground heat flux for different organic layer depths

Using the calibrated model, an investigation into the influence of climate warming on the active layer was conducted by comparing the simulated soil temperature profiles in two scenarios for changing mean annual air temperature (Fig. 12). It is found that the maximum active layer thickness at Tanggula observation site may increase by approximately 30 cm and 60 cm compared to the current 330 cm active layer thickness, depending on whether an air temperature increase of 1℃ or 2℃, respectively. The simulated monthly average ground heat flux had a tendency to increase from March to September (Fig. 13), which indicates that the energy increased from the atmosphere into the soil. The amplitude was 8.49 w/m^2 and 26.50 w/m^2 in 2009–2012 when the air temperature increased 1℃ and 2℃, respectively. From October to the following February, a reverse trend was measured; the reduction is 5.92 w/m^2 and 7.89 w/m^2 in 2009−2012 when the air temperature under similar changes. This energy change is mainly due to an increase in the active layer thickness; and these data further shows that permafrost is degrading as the global climate warms.

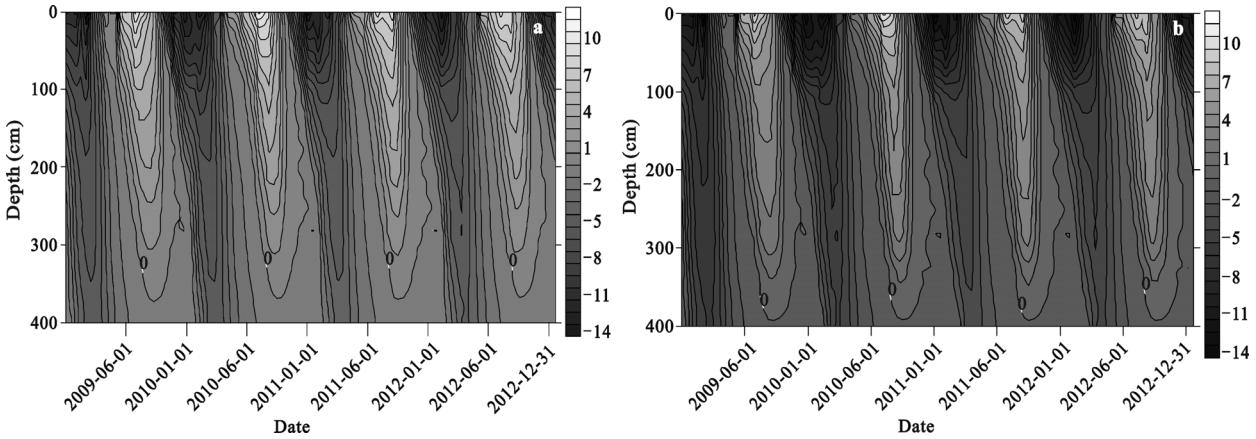

Fig. 12 Simulated soil temperature (℃) for two climate change scenarios. Scenario1: increasing air temperature by 1℃ (a); scenario2: increasing air temperature by 2℃ (b)

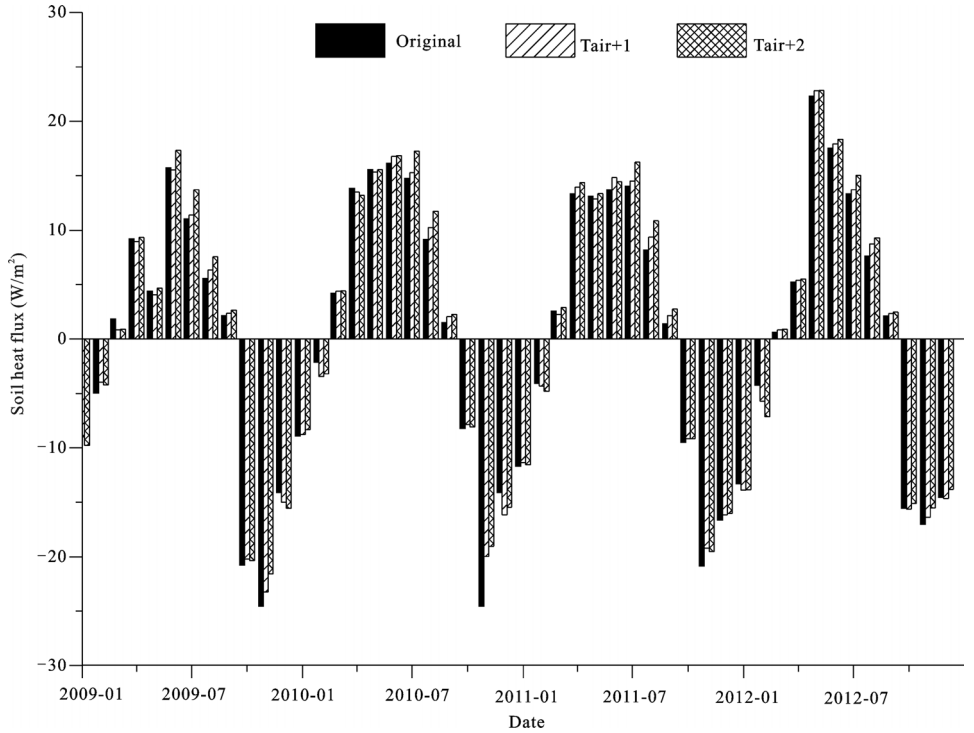

Fig. 13 Simulated monthly average ground heat flux for different climate change scenarios. Tair+1: air temperature increase 1℃; Tair+2: air temperature increase 2℃

5 Discussion

In this study, the CoupModel performed well in simulating the soil temperature and moisture at the Tanggula observation site in the permafrost region, although there were some discrepancies between the unfrozen water content of the simulated soil and the measured values. As expected, larger discrepancies were found between the simulated and measured water content in the upper 20 cm of the soil. The reason may be that the water content of the soil surface is influenced by precipitation and other factors; and it was extremely sensitive to climate changes. In addition, the parameters for the vegetation were empirical coefficients, resulting in inadequate consideration of the water absorption by vegetation and other aspects. Some of the discrepancies between the simulated and measured water content at the beginning of the thawing period might be due to inaccurate observations due to improper instrument calibration. As the depth increased, the simulation accuracy improved, which may be related to the distance from the natural ground surface.

The results from Yang *et al.* (2010) showed that the downward heat process becomes more active during the thawing period, and there is no confinement of the melt water in the thawing front on the alpine meadow frozen grounds of the source area of the Heihe River. The results of this study confirmed that conclusion. We also found that the soil layers have a steady soil heat flux that is near zero during the thawing to freezing stage and the reverse process. The initial water content and soil organic layer affect the thickness of the active layer. Zhou *et al.* (2013) found that the maximum thawing depth in summer may increase from 150 cm with realistic 40 cm organic layer to almost 300 cm as a result of ignoring the organic soil layer and decrease almost 50 cm from 40 cm to 80 cm organic soil layer. In this study, the maximum thawing depth for the active layer in summer is close to 330 cm when the organic layer is 0 cm. However, it is lower than 280 cm and 250 cm with organic layer depths of 20 cm and 40 cm, respectively. The results also reveal that the soil organic layer reduces the response of the active layer to external factors and contributes to the conservation of permafrost. We also found that higher initial water content delays and reduces the soil heat flux transfer.

The results of this study reveals that the maximum active layer thickness at Tanggula observation site may increase by approximately 30 cm and 60 cm compared to the current 330 cm active layer thickness, depending on whether an air temperature increase of 1℃ or 2℃, respectively. The measured evidence shows that the permafrost has been warming, thawing, and degrading over the past few decades on the Qinghai-Tibet Plateau (Cheng and Wu, 2007; Wu and Zhang, 2008), and the active thickness has deepened by 10–40 cm from 1995 to 2004 in permafrost regions (Wu and Liu, 2004; Yang *et al*., 2004; Wu *et al*., 2006). Meanwhile, the air temperature increased 0.25℃/10yr from 1961 to 2002 on the Qinghai-Tibet Plateau (Wang *et al*., 2005). The simulated result also demonstrated that climate warming will cause the permafrost active layer to deepen and change, consistent with the measured evidence.

6 Conclusions

This study applied the CoupModel for fully coupled heat transport and water flow for permafrost regions. The model results demonstrated that the CoupModel can describe the hydrothermal transfer processes. Based on the calibrated model, an analysis with respect to the influence of the initial water content and the organic soil layer depth on the active layer was performed. The model was used to predict the changes in the active layer as a response to 0, 15% and 20% initial moisture content. The results show that higher moisture content delays the soil heat flux transfer. The maximum thawing depth in summer may decrease from 330 cm with no organic layer to almost 280 cm and 250 cm as a result of 20 cm and 40 cm organic soil layers, respectively. It indicated that the organic soil layers reduce the rate of the active layer deepening under future climate warming. An analysis with respect to the influence of climate warming on the active layer was performed. Using the model to predict the changes in the active layer in response to a 1℃ and 2℃ warming indicates that the maximum active layer thickness may increase from 330 cm at present to approximately 360 cm and 390 cm as a result of 1℃ and 2℃ warming, respectively. These results indicated that climate warming will cause the permafrost active layer to deepen.

In summary, the CoupModel can be used to simulate the water-heat characteristics of soil in the active layer in permafrost regions with higher elevations, such as the

Qinghai-Tibet Plateau in China. The results reveal that air temperature is more important than precipitation in terms of the behavior of permafrost under different climate-change conditions. When the climate warms, the maximum active layer thickness becomes deeper, but the impact on the layer thickness is not obvious with increased precipitation. In future work, it would be of value to test the ability of CoupModel to simulate similar conditions for more complex systems, including dynamic vegetation and soil surface snow cover.

Acknowledgments

We thank Cryosphere Research Station on the Tibet Plateau, Chinese Academy of Sciences for providing data and other help.

References

Alexeev V A, Nicolsky D J, Romanovsky V E *et al*., 2007. An evaluation of deep soil configurations in the CLM3 for improved representation of permafrost. *Geophysical Research Letters*, 34(9): L090502. doi: 10.1029/2007GL029536

Bowling L C, Lettenmaier D P, Nijssen B *et al*., 2003. Simulation of high-latitude hydrological processes in the Torne-Kalix Basin: PILPS phase 2(e)3: Equivalent model representation and sensitivity experiments. *Global and Planetary Change*, 38(1–2): 55–71. doi: 10.1016/S0921-8181(03)00005-5

Cheng G D, Wu T H, 2007. Responses of permafrost to climate change and their environment significance, Qinghai-Tibet Plateau. *Journal of Geophysical Research*, 112 (F2): F02S03. doi: 10.1029/2006JF000631

Cheng Guodong, 1990. Recent development of geocryological study in China. *Acta Geographica Sinica*, 45(2): 220–223. (in Chinese)

Cheng Guodong, 1998. Glaciology and geocryology of China in the past 40 years: Progress and prospect. *Journal of Glaciology and Geocryology*, 20(3): 213–226. (in Chinese)

Cheng Guodong, Zhao Lin, 2000. The problems associated with permafrost in the development of the Qinghai-Xizang Plateau. *Quaternary Sciences*, 20(6): 521–531. (in Chinese)

Eckersten H, Blomback K, Katterer T *et al*., 2001. Modelling C, N, water and heat dynamics in winter wheat under climate change in southern Sweden. *Agriculture Ecosystems & Environment*, 86(3): 221–235. doi: 10.1016/S0167-8809(00)00284-X

Gao Z Q, Chae N, Kim J *et al*., 2004. Modeling of surface energy partitioning, surface temperature and soil wetness in the Tibet prairie using the simple biosphere model 2(SiB2). *Journal of Geophysical Research*, 102(D06): 1–11. doi: 10.1029/2003JD 004089

Harlan R L, 1973. Analysis of coupled heat-fluid transport in partially frozen soil. *Water Resources Research*, 9(5): 1314–1323. doi: 10.1029/WR009i005p01314

He Ping, Cheng Guodong, Zhu Yuanlin, 2001. The progress of study on heat and mass transfer in freezing soils. *Journal of Glaciology and Geocryology*, 23(1): 92–98. (in Chinese)

Henderson-Sellers A, Pitman A J, Love P K *et al*., 1995. The project for intercomparison of land-surface parameterization schemes (PILPS)-phase-2 and phase-3. *Bulletin of the American Meteorological Society*, 76(4): 489–503.

Henderson-Sellers A, Yang Z L, Dickinson R E, 1993. The project for intercomparison of land-surface parameterization schemes. *Bulletin of the American Meteorological Society*, 74(7): 1335–1350.

Jansson P E, Karlberg L, 2004. Theory and practice of coupled heat and mass transfer model for soil-plant-atmosphere system. In: Zhang Hongjiang *et al*. (eds.). *Translation.* Beijing: Science Press, 1–50. (in Chinese)

Jansson P E, Moon D, 2001. A coupled model of water, heat and mass transfer using object orientation to improve flexibility and functionality. *Environmental Modelling & Software*, 16(1): 37–46. doi: 10.1016/S1364-8152(00)00062-1

Li X, Cheng G D, Jin H J *et al*., 2008. Cryospheric change in China. *Global and Planetary Change*, 62: 210–218.

Loumagne C, Chkir N, Normand M, 1996. Introduction of the soil vegetation-atmospheric continuum in a conceptual rainfall-runoff model. *Hydrological Science Journal*, 41(6): 889–902.

Luo Jinming, Deng Wei, Zhang Xiaoping *et al*., 2008. Variation of water and salinity in sodic saline soil during frozen-thawing season. *Advances in Water Sciences*, 19(4): 559–566. (in Chinese)

Luo Siqiong, Lv Shihua, Zhang Yu *et al.*, 2008. Simulation analysis on land surface process of BJ site of central Tibet Plateau using CoLM. *Plateau Meteorology*, 27(2): 259–271. (in Chinese)

Mao Xuesong, Hu Changshun, Dou Mingjian *et al*., 2003. Dynamic observation and analysis of moisture and temperature field coupling process in freezing soil. *Journal of Glaciology and Geocryology*, 25(1): 55–59. (in Chinese)

McGechan M B, Graham R, Vinten A J A *et al*., 1997. Parameter selection and testing the soil water model SOIL. *Journal of Hydrology*, 195(1–4): 312–334.

Nassar I N, Horton R, Flerchinger G N, 2000. Simultaneous heat and mass transfer in soil columns exposed to freezing/thawing conditions. *Soil Science*, 165(3): 208–216.

Nicolsky D J, Romanovsky V E, Alexeev V A *et al*., 2007. Improved modeling of permafrost dynamics in a GCM land surface scheme. *Geophysical Research Letters*, 34(8): L080501. doi: 10.1029/2007GL029525

Riseborough D W, Shiklomanov N I, Etzelmuller B *et al*., 2008. Recent advances in permafrost modeling. *Permafrost and Periglacial Processes*, 19(2): 137–156. doi: 10.1002/ ppp.615

Scherler M, Hauck C, Hoelzle M *et al*., 2010. Melt water infiltration into the frozen active layer at an Alpine permafrost site. *Permafrost and Perglacial Process*, 21(4): 325–334.

Shoop S A, Bigl S R, 1997. Moisture migration during freeze and thaw of unsaturated soils: Modeling and large scale experiments. *Cold Regions Science and Technology*, 25(1): 33–45. doi: 10.1016/S0165-232X (96)00015-8

Wang Chenghai, Shi Rui, 2007. Simulation of the land surface processes in the western Tibet Plateau in summer. *Journal of Glaciology and Geocryology*, 29(1): 73–81. (in Chinese)

Wang Qingchun, Li Lin, Li Dongliang *et al*., 2005. Response of permafrost over Qinghai Plateau to climate warming. *Plateau Meteorology*, 24(5): 708–713. (in Chinese)

Wu Q B, Cheng G D, Ma W *et al*., 2006. Technical approaches on permafrost thermal stability for Qinghai-Tibet Railway. *Geomechanics and Geoengineering*, 1(2): 119–127. doi: 10.1080/17486020600777861

Wu Q B, Liu Y J, 2004. Ground temperature monitoring and its recent change in Qinghai-Tibet Plateau. *Cold Regions Science and Technology*, 38(2–3): 85–92. doi: 10.1016/S0165-232X (03)00064-8

Wu Q B, Zhang T J, 2008. Recent permafrost warming on the Qinghai-Tibet Pleateau. *Journal of Geophysical Research*, 113: D13108.

Wu Qingbai, Shen Yongping, Shi Bin, 2003. Relationship between frozen soil together with its water-heat process and ecological environment in the Tibet Plateau. *Journal of Glaciology and Geocryology*, 25(3): 250–255. (in Chinese)

Wu S H, Jansson P E, Zhang X Y, 2011a. Modeling temperature, moisture and surface heat balance in bare soil under seasonal frost conditions in China. *European of Journal of Soil Science*, 62(6): 780–796. doi: 10.1111/j. 1365-2389.2011.01397.x

Wu S H, Jansson P E, Kolari P, 2012. The role of air and soil temperature in the seasonality of photosynthesis and transpiration in a boreal scots pine ecosystem. *Agricultural and Forest Meteorology*, 156: 85–103. doi: 10.1016/j.agrformet.2012.01.006

Xiao Y, Zhao L, Dai Y J *et al*., 2013. Representing permafrost properties in CoLM for the Qinghai-Xizang (Tibet) Plateau. *Cold Regions Science and Technology*, 87(4): 68–77. doi: 10.1016/j.coldregions.2012.12.004

Xiao Yao, Zhao Lin, Li Ren *et al*., 2011. Seasonal variation characteristics of surface energy budget components in permafrost regions of northern Tibet Plateau. *Journal of Glaciology and Geocryology*, 33(5): 1033–1037. (in Chinese)

Xu Xuezu, Wang Jiacheng, Zhang Lixin, 2001. *Physics of Frozen Soils*. Beijing: Science Press, 1–30. (in Chinese)

Yang Jianping, Ding Yongjian, Chen Rensheng *et al*., 2004. Permafrost change and its effect on eco-environment in the source regions of the Yangtze and Yellow Rivers. *Journal of Mountain Science*, 22(3): 278–285. (in Chinese)

Yang Meixue, Yao Tandong, 1998. A review of the study on the impact of snow cover in the Tibet an Plateau on Asian Monsoon. *Journal of Glaciology and Geocryology*, 20(2): 14–19. (in Chinese)

Yang Yong, Chen Rensheng, Ji Xibin *et al*., 2010. Heat and water transfer processes on alpine meadow frozen grounds of Heihe mountainous in Northwest China. *Advances in Water Science*, 21(1): 30–34. (in Chinese)

Yao J M, Zhao L, Ding Y J *et al*., 2008. The surface energy budget and evapotranspiration in the Tanggula region on the Tibet Plateau. *Cold Regions Science and Technology*, 52(1): 326–340. doi: 10.1016/j.coldregions.2007.04.001

Zhang S L, Lövdahl L, Grip H *et al*., 2007. Modelling the effects of mulching and fallow cropping on water balance in the Chinese Loess Plateau. *Soil & Tillage Research*, 100(2–3): 311–319. doi: 10.1016/j.fcr.2006.08.006

Zhang Yanwu, Lv Shihua, Li Dongliang *et al*., 2003. Numerical simulation of freezing soil process on Qinghai-Xizang Plateau in early winter. *Plateau Meteorology*, 22(5): 471–477. (in Chinese)

Zhang Yu, Song Meihong, Lv Shihua *et al.*, 2003. Frozen soil parameterization scheme coupled with mesoscale model. *Journal of Glaciology and Geocryology*, 25(5): 541–546. (in Chinese)

Zhao Lin, 2004. *The Freezing-thawing Processes of Active Layer and Changes of Seasonally Frozen Ground on the Tibet Plateau*. Beijing: Chinese Academy of Sciences, 30–50. (in Chinese)

Zhao Lin, Li Ren, Ding Yongjian, 2008. Simulation on the soil water-thermal characteristics of the active layer in Tanggula range. *Journal of Glaciology and Permafrost Engineering*, 30(6): 930–937. (in Chinese)

Zhou J, Kinzelbach W, Cheng G D *et al*., 2013. Monitoring and modelling the influence of snow pack and organic soil on a permafrost active layer, Qinghai-Tibet Plateau of China. *Cold Regions Science and Technology*, 90–91: 38–52. doi: 10.1016/j.coldregions.2013.03.003